Relationships among Pore Size, Connectivity, Dimensionality of Capillary Condensation, and Pore Structure Tortuosity of Functionalized Mesoporous Silica

ARTICLE *in* LANGMUIR · MARCH 2003

Impact Factor: 4.46 · DOI: 10.1021/la020261h

5 AUTHORS, INCLUDING:

Constantinos Salmas
National Technical University of Athens
32 PUBLICATIONS **422** CITATIONS
SEE PROFILE

Maria Louloudi
University of Ioannina
76 PUBLICATIONS **971** CITATIONS
SEE PROFILE

Relationships among Pore Size, Connectivity, Dimensionality of Capillary Condensation, and Pore Structure Tortuosity of Functionalized Mesoporous Silica

G. S. Armatas,[†] C. E. Salmas,[‡] M. Louloudi,[†] G. P. Androutsopoulos,[‡] and P. J. Pomonis*,[†]

Department of Chemistry, University of Ioannina, Ioannina 45 110, Greece, and Department of Chemical Engineering, National Technical University of Athens, GR Athens 15 780, Greece

Received March 15, 2002. In Final Form: November 11, 2002

Seven mesoporous forms of silica were prepared by controlled and gradual functionalization of the original SiO_2 surface with silano-(trimethoxy)-propyl-imidazole groups. The degree of surface functionalization was $n = 0.00$, 0.23, 0.30, 0.40, 0.52, 0.60, and 0.85 and was controlled by previous knowledge of surface acidity, determined by temperature-programmed desorption of NH_3. From N_2 adsorption/desorption measurements, the specific surface area S_p ($m^2\ g^{-1}$), the specific pore volume V_p ($cm^3\ g^{-1}$), and the corresponding pore size distributions (PSDs) were determined. The connectivity c of the solids was also calculated according to the method of Seaton, and the dimensionality of capillary condensation D_{cc} was found using the thermodynamic method of Neimark. The increase of functionalization resulted in a linear drop of S_p and V_p, and the maximum D_{max} of the PSD and the full width at half-maximum, fwhm $\sim 2\sigma$, of the distribution drop in a regular way whereas the ratio ($D_{max}/2\sigma$) remains practically constant. The connectivity c also decreases from $c = 12.5$ at $n = 0$ to $c = 3$ at $n = 0.60-0.85$, presumably because of blocking of channels connecting various pores. The D_{cc} values decrease with increasing n values. Next, the co-called corrugated pore structure model, CPSM, was employed for the estimation of tortuosity τ of the porous solids and the simulation of the experimental adsorption/desorption isotherms. From those CPSM simulations, the corresponding specific surface area S_{CPSM} ($m^2\ g^{-1}$), the specific pore volume V_{CPSM} ($cm^3\ g^{-1}$), and the corresponding pore size distribution PSD_{CPSM} were estimated. The tortuosity τ of the system drops with the degree of functionalization from $\tau = 4.22$ at $n = 0$ to $\tau = 3.37$ at the initial functionalization ($n = 0.23$) and subsequently remains practically constant at about $\tau = 3.40 \pm 0.10$, for the same reasons which affect the connectivity, that is, blocking of various pore channels. The comparison between the parameters V_p and V_{CPSM} is quite satisfactory. The S_{CPSM} values appear systematically higher by 8−23% compared to the S_p ones. The dimensionality of capillary condensation D_{cc} is related to the variance 2σ of the PSD. The reasons and the limits of this relationship are discussed.

Introduction

The most common kind of porous materials are the ones possessing a disordered or random porous network.[1,2] In this class of solids belong various silicas,[3] aluminas,[4] aluminophosphates,[5] and a large number of aluminosilicate solids encountered in geological forms.[6] The pore size distribution of such disordered or random porous materials is usually characterized on a routine basis by N_2 adsorption at 77 K. From such measurement, the following characteristic parameters of porous solids can be calculated:

The Specific Surface Area S_p ($m^2\ g^{-1}$) and the Specific Pore Volume V_p ($cm^3\ g^{-1}$).[1,2,7] These parameters are the most usual ones giving a fair idea about the kind of porous materials at hand but also helping in the calculation of surface reaction rates per m^2 and for the estimation of adsorption capacity per gram of solid.

The Maximum of the Pore Size Distribution (PSD) Curve, D_{max} (nm), and the Variance of Distribution 2σ (nm). These parameters are important since they express the maximum and the narrowness of the PSD, which can be related to the sieving capacity of the porous materials. The ratio of those two terms $D_{max}/2\sigma$ is also very informative about the relative narrowness of distribution, which is extremely useful in chromatographic separations.

The Pore Connectivity c. This parameter, which might be critical in understanding and describing porous systems, is not commonly determined by workers in the field. One of the reasons is that until the 1990s there was not a tractable and acceptable method to find c. Today, thanks to the work of Seaton[8] there is such a methodology, while Liapis and co-workers have also provided an alternative method.[9] The practical use of c is that it can be helpful in deciding about the choice of porous materials

* Corresponding author. Tel: +30651 98350. Fax: +30651 98795. E-mail: ppomonis@cc.uoi.gr.

[†] University of Ioannina.

[‡] National Technical University of Athens.

(1) Gregg, S. J.; Sing, K. S. W. *Adsorption, Surface Area and Porosity*, 2nd ed.; Academic Press: London, 1982.

(2) Rouquerol, F.; Rouquerol, J.; Sing, K. S. W. *Adsorption by Powders and Porous Solids*; Academic Press: San Diego, 1999.

(3) Brinker, C. J.; Scherer, G. W. *Sol−Gel Science*: *The Physics and Chemistry of Sol−Gel Processing*; Acedemic Press: New York, 1990.

(4) Trimm, D. L.; Stanislaus, A. *Appl. Catal.* **1986**, *21*, 215.

(5) (a) Oliver, S.; Kuperman, A.; Ozin, G. A. *Angew. Chem., Int. Ed.* **1998**, *37*, 46. (b) Oliver, S.; Kuperman, A.; Coomds, N.; Lough, A.; Ozin, G. A. *Nature* **1995**, *378*, 47.

(6) (a) *Pillared Layered Structures*: *Current Tends and Applications*; Mitchel, I. V., Ed.; Elsevier Applied Science: Amsterdam, 1990. (b) Barrer, M. R. *Zeolites and Clay Minerals as Sorbents and molecular Sieves*; Academic Press: New York, 1978.

(7) Lowell, S. *Introduction to Powder Surface Area*; John Wiley and Sons: New York, 1979.

(8) (a) Seaton, N. A. *Chem. Eng. Sci.* **1991**, *46*, 1895. (b) Liu, H.; Zhang, L.; Seaton, N. A. *Chem. Eng. Sci.* **1992**, *47*, 4393. (c) Liu, H.; Zhang, L.; Seaton, N. A. *J. Colloid Interface Sci.* **1993**, *156*, 285. (d) Liu, H.; Zhang, L.; Seaton, N. A. *Langmuir* **1993**, *9*, 2576. (e) Liu, H.; Seaton, N. A. *Chem. Eng. Sci.* **1994**, *49*, 1869.

(9) (a) Meyers, J. J.; Nahar, S.; Ludlow, D. K.; Liapis, A. I. *J. Chromatogr. A* **2001**, *907*, 57. (b) Meyers, J. J.; Liapis, A. I. *J. Chromatogr. A* **1998**, *827*, 197.

10.1021/la020261h CCC: $25.00
Published on Web 03/13/2003

in separation processes.[9] We also mentioned that the connectivity c can be parallelized to the branching ratio $\sim b$ of trees.[10] A comparison between those parameters c and b reveals some very interesting topological heterosimilarities between the pore network in a solid and the branching of trees.

The Tortuosity of Pores τ. This is a difficult property to estimate, and it is often considered as a correction factor to various model deficiencies. According to the words of Aris,[11] "When models are made of the configuration of pore structure, τ, can be related to some other geometrical parameters but in general it is a fudge factor of greater or less sophistication". Tortuosity is traditionally[12] regarded as a function of a *pore length (or angle) factor L and a pore shape factor S*:

$$\tau = f(L, S) \tag{1}$$

Factor L accounts for the longer distance that a diffusing species has to travel through a real pore channel connecting two fixed points within the particle, compared to the straight distance between the points. The shape factor S reflects the effect of pore cross-sectional area variation along the pore length upon the diffusion process.[12] Tortuosity factors are normally greater than unity. The experimental determination of τ necessitates measurements of effective diffusivities D_{eff} in a Wicke−Kallenbach cell and then use of the formula

$$D_{\text{eff}} = \frac{D_{\text{b}}\epsilon}{\tau} \tag{2}$$

where D_{b} stands for the binary diffusion coefficient and ϵ is the voidage fraction. Details on how eq 2 can be employed are cited in ref 13. Numerous τ values for a variety of materials are reported in ref 12. The first attempt to estimate tortuosity factors without the execution of diffusion measurements was made by Carniglia[14] who used data from Hg porosimetry. But a drawback of that method is that it does not take into account the mesopore and micropore regions, which are not traced by mercury porosimetry. Nevertheless, recently Androutsopoulos and Salmas proposed a method that enables the prediction of tortuosities τ in porous solids from N_2 adsorption−desorption measurements.[15] This method is based on the so-called corrugated pore structure model (CPSM), suitable for the simulation of all types of adsorption/desorption hysteresis loops.[16]

The Dimensionality of Adsorption D. This quantity can be calculated by the thermodynamic method of Neimark[17] employing the relationship

$$\log S = \text{constant} + (D - 2)\log r \tag{3}$$

Another method, less often used for the estimation of dimensionality of adsorption, is the modified Frenkel−Hill−Halsey equation.[18]

Although the two methods are equivalent to each other at low pressures as shown recently by various groups,[19] the first one provides much richer information, *provided that we extend its application to the range of* (P/P_0) *where capillary condensation takes place.* Thus, as has been shown previously[10,20] at low (P/P_0) the dimensionality of adsorption as found by eq 3 is around 2 and corresponds practically to the fractal dimensionality of the surface as "seen" by the adsorbed species. This value will be designated in the text as D_{sa} meaning dimensionality of surface adsorption. But at higher (P/P_0) values, where condensation takes place, the log S versus log r plots result in slopes which provide D values between 4 and 10. These values will be designated in the text as D_{cc} meaning dimensionality of capillary condensation. It was suggested that such high D_{cc} values actually correspond to the clustering of N_2 molecules during their supercritical condensation into the pores.[10,20] In this work, we are interested in this last parameter D_{cc}.

Now an important question is, how are those parameters S_{p}, V_{p}, $(D_{\max}/2\sigma)$, c, τ, and D_{cc} affected by the gradual narrowing of pores due to some kind of surface functionalization? A second objective is to examine which of, and how, the parameters τ, c, D_{cc}, and $(D_{\max}/2\sigma)$ are interrelated. The question becomes more interesting, and perhaps intriguing, since all the above quantities are calculated just from one kind of measurement, namely, the N_2 adsorption/desorption data. A partial answer to the above question was attempted in a previous work[10] in which 16 mesoporous vanado-phosphoro-aluminate solids were tested and some relationships between c, D_{cc}, and $(D_{\max}/2\sigma)$ were established. A first target of this paper is to extend the search for such possible interrelations to a class of mesoporous silicas, with a random pore size distribution whose porosity has been systematically and gradually modified by surface functionalization using silano-(trimethoxy)-propyl-imidazole (STPI) groups as surface modification agents.

A third objective is to compare the parameters S_{CPSM} and V_{CPSM} calculated via the CPSM simulations to the corresponding ones S_{p} and V_{p} found by the more standard methods. The materials used for testing were seven samples of commercial SiO_2 with a degree of surface functionalization equal to $n = 0.00$, 0.23, 0.30, 0.40, 0.52, 0.60, and 0.85.

Experimental Section

Preparation of Samples. Seven samples, based on a commercial SiO_2, were prepared with gradual functionalization of its acid sites with a STPI groups. The extent of functionalization was controlled to $n = 0.00$, 0.23, 0.30, 0.40, 0.52, 0.60, and 0.85 as follows in the preparation procedures. Commercial silica of 60−80 mesh (Davison grade 59) was dried in the oven at 150 °C and refluxed in toluene with the estimated amount of imidazole and redistilled 3-chloropropyl-trimethoxy-silane (ClPTMS). Different degrees of coverage were obtained by varying the concentration of reagents and the time of reflux from 2 to 12 h. The relevant reactions which took place are shown schematically

(10) Pomonis, P. J.; Kolonia, K. M.; Armatas, G. S. *Langmuir* **2001**, *17* (26), 8397.
(11) Aris, R. *The Mathematical Theory of Diffusion and Reaction in Permeable Catalysis*; Clarendon Press: Oxford, 1975; Vol. 1, p 25.
(12) Satterfield, C. N. *Mass Transfer in Heterogeneous Catalysis*; M.I.T. Press: Cambridge, MA, 1970.
(13) Salmas, C. E.; Stathopoulos, V. N.; Pomonis, P. J.; Androutsopoulos, G. P. *Langmuir* **2002**, *18*, 423.
(14) Carniglia, S. C. *J. Catal.* **1986**, *102*, 401.
(15) Salmas, C. E.; Androutsopoulos, G. P. *Ind. Eng. Chem. Res.* **2001**, *40*, 721.
(16) (a) Androutsopoulos, G. P.; Salmas, C. E. *Ind. Eng. Chem. Res.* **2000**, *39*, 3747. (b) Androutsopoulos, G. P.; Salmas, C. E. *Ind. Eng. Chem. Res.* **2000**, *39*, 3764.
(17) (a) Neimark, A. V.; Unger, K. K. *J. Colloid Interface Sci.* **1993**, *412*, 2649. (b) Neimark, A. V. *Physica A* **1992**, *191*, 258. (c) Neimark, A. V.; Hanson, M.; Unger, K. K. *J. Phys. Chem.* **1993**, *97*, 6011.
(18) (a) Avnir, D.; Jaroniec, M. *Langmuir* **1989**, *5*, 1431. (b) Pfeifer, P.; Cole, W. M. *New J. Chem.* **1990**, *14*, 221. (c) Pfeifer, P.; Odert, M.; Cole, W. M. *Proc. R. Soc. London, Ser. A* **1989**, *423*, 169. (d) Pfeifer, P.; Wu, J. Y.; Cole, W. M.; Krim, J. *Phys. Rev. Lett.* **1989**, *62*, 1997. (e) Yin, Y. *Langmuir* **1991**, *7*, 216. (f) Neimark, A. V. *JETP Lett.* **1990**, *51*, 607.
(19) (a) Jaroniec, M. *Langmuir* **1995**, *11*, 2316. (b) Sahouli, B.; Blackev, S.; Browery, F. *Langmuir* **1996**, *12*, 2872.
(20) Petrakis, D. E.; Pashalidis, I.; Theoharis, E. R.; Hudson, M. J.; Pomonis, P. J. *J. Colloid Interface Sci.* **1997**, *185*, 104.

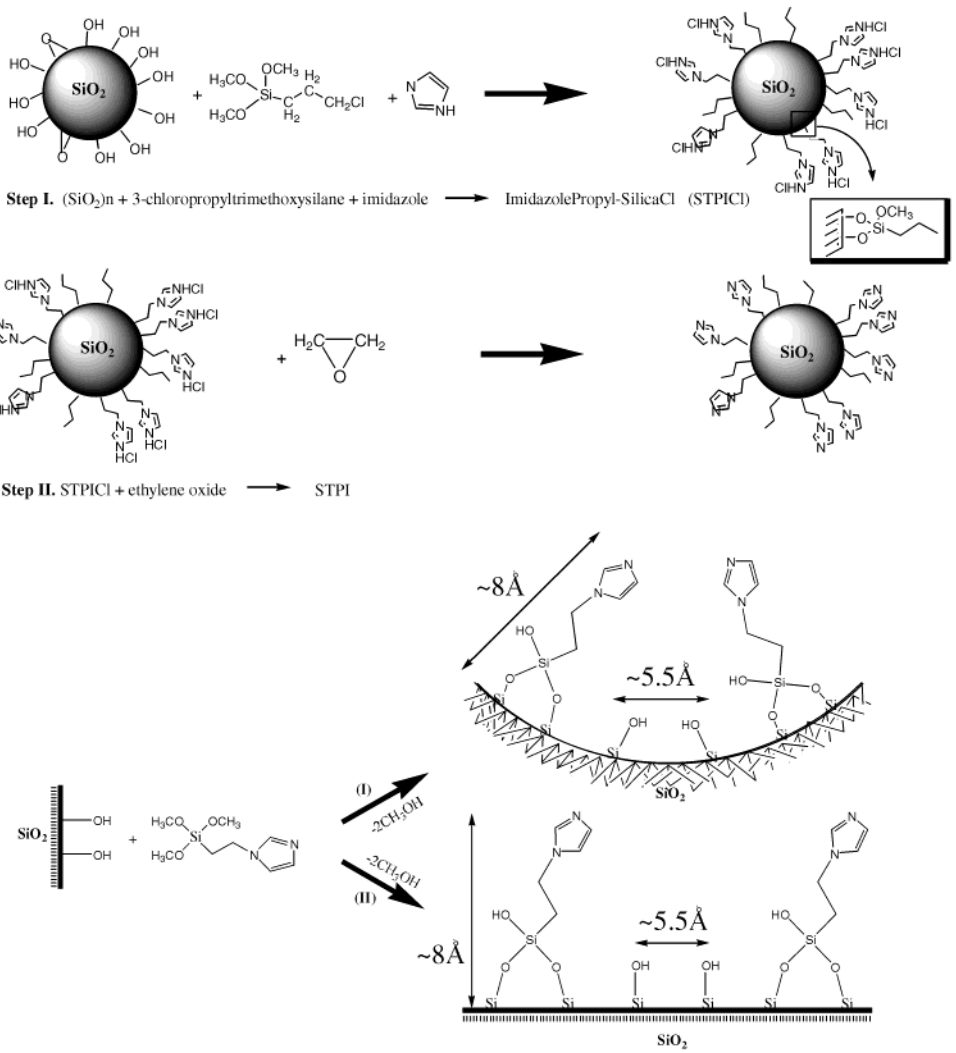

Figure 1. Schematic reaction pathways for the functionalization of the acid sites of SiO_2 with STPI groups. In the lower part, the length of the functionalizing STPI groups is ascribed to be ~8 Å, while the distance between the acid sites of SiO_2 is mentioned to be around ~5.2 Å.

Table 1. Samples of Functionalized SiO_2 Prepared and Their Specific Surface Areas (S_p) and Specific Pore Volumes (V_p)[a]

sample	S_p (BET) (m_2 g^{-1})	V_p (cm^3 g^{-1})	D_{max} (nm)	fwhm = 2σ (nm)	$D_{max}/2\sigma$
SiO_2[b]	279	1.14	14.25	8.30	1.72
$SiO_2(STPI)_{0.23}$	255	0.92	12.41	6.45	1.92
$SiO_2(STPI)_{0.30}$	242	0.95	12.44	5.90	2.11
$SiO_2(STPI)_{0.40}$	244	0.82	12.47	6.90	1.81
$SiO_2(STPI)_{0.52}$	232	0.81	14.88	2.60	5.72
$SiO_2(STPI)_{0.60}$	227	0.88	12.07	7.25	1.66
$SiO_2(STPI)_{0.85}$	209	0.77	12.78	6.75	1.89

[a] The maximum D_{max} of the PSD, the variance 2σ of the distribution, and the ratio $D_{max}/2\sigma$ are also mentioned. n = 0.23, 0.30, 0.40, 0.52, 0.60, and 0.85, where n = mmoles (STPI) added/mmoles of acid sites (NH_3 TPD). [b] Total surface acidity (NH_3 TPD) = 12.81×10^{20} acid sites/g.

in Figure 1. The obtained solids with some of their properties are listed in Table 1.

Surface Acidity Measurements. To enable the controlled addition of STPI groups on the acid sites of the silica surface, its total (Lewis + Brønsted) acidity was determined using NH_3 adsorption in a standard temperature-programmed desorption (TPD) apparatus similar to that described.[21] Briefly, the procedure was the following. The sample weighing about 200 mg was put on the perforated bed of a silica tube with a diameter of 1 cm. The tube was connected to a gas chromatograph (Shimadzu GC-8A) with a TC detector. Each sample was initially heated at 500 °C in a flow of helium for 2 h, whereupon the temperature was reduced to the working level of 100 °C. Then the sample was saturated with dried ammonia by replacing, for 30 min, the flow of helium through the sample by a flow of dried ammonia. The weakly adsorbed ammonia was flushed out with helium flow (50 mL min^{-1}) for 2 h at 110 °C. After stripping of the weakly adsorbed ammonia, the sample was cooled to 100 °C and heating was begun at a rate of 10 °C min^{-1} till 500 °C where it remained for 2 h. The amount of ammonia eluted was trapped in a bubble bottle, which contained an excess of 0.01 N hydrochloric acid solution. The trapped ammonia was determined by volumetric titration of the excess HCl using 0.05 N NaOH. Knowing the exact number of acid sites per gram of SiO_2, it was possible to control the addition of STPI groups by the corresponding amount added in the preparation beaker.

Surface Area and Porosity. A Fisons Sorptomatic 1900 instrument was used to carry out pore size distribution measurements. The characterization techniques included the determination of nitrogen adsorption−desorption isotherms at 77 K. Prior to each experiment, the samples were degassed at 250 °C in a vacuum of 5×10^{-2} mbar for 12 h. The desorption branch

(21) (a) Sklari, S.; Rahiala, H.; Stathopoulos, V.; Rosenform, J.; Pomonis, P. J. *Microporous Mesoporous Mater.* **2001**, *49*, 1. (b) Stathopoulos, V. N.; Ladavos, A. K.; Kolonia, K. M.; Skaribas, S. D.; Petrakis, D. E.; Pomonis, P. J. *Microporous Mesoporous Mater.* **1999**, *31*, 111. (c) Ladavos, A. K.; Trikalitis, P. N.; Pomonis, P. J. *J. Mol. Catal. A: Chem.* **1996**, *106*, 241.

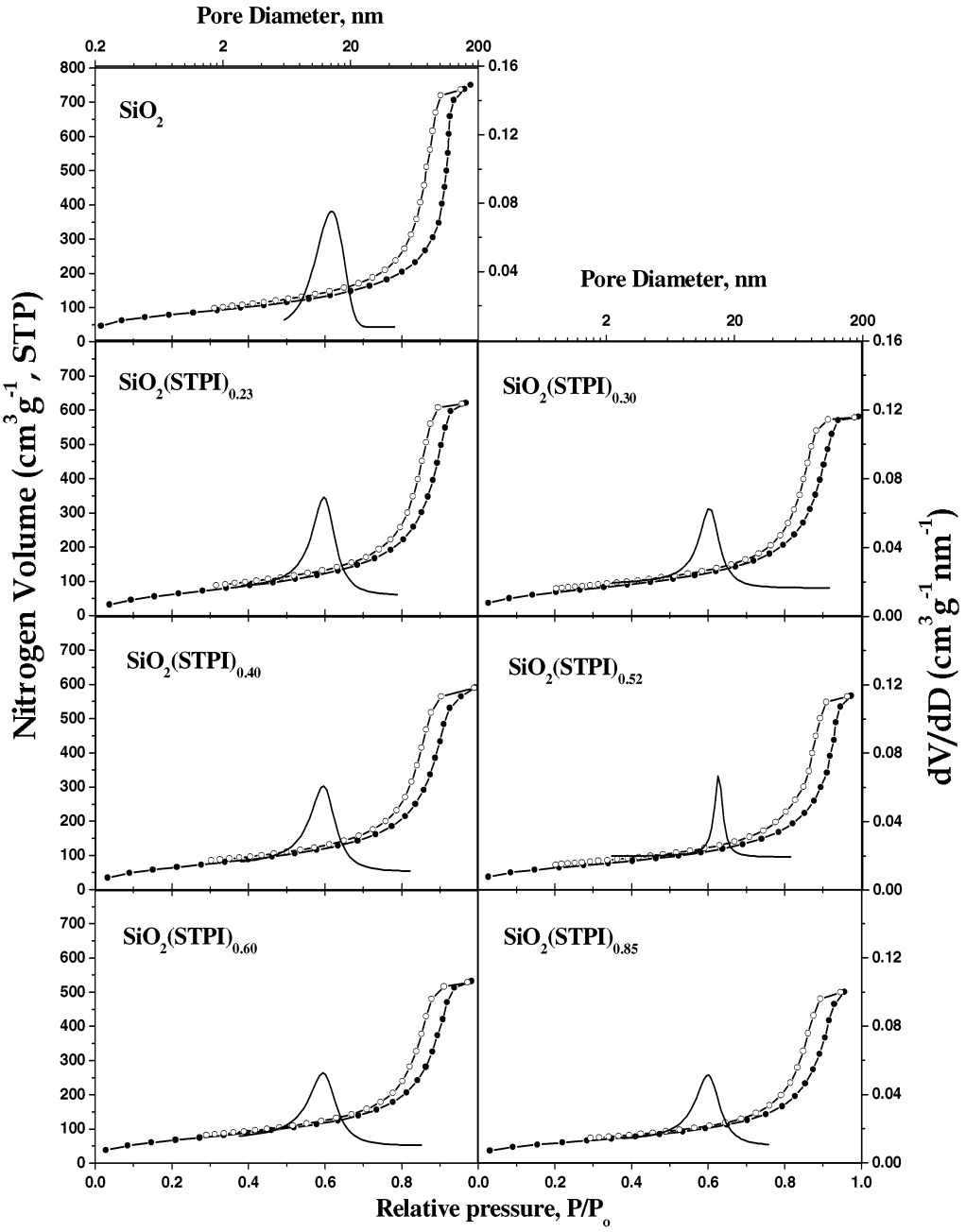

Figure 2. Nitrogen adsorption−desorption isotherms at 77 K and the corresponding PSD curves calculated from the desorption branch.

of the isotherms was used for the calculation of the PSD and is shown in Figure 2. The specific surface area of the sample was calculated by applying the Brunauer−Emmett−Teller (BET) equation using the linear part ($0.05 < P/P_0 < 0.30$) of the adsorption isotherm and assuming a closely packed BET monolayer. The calculated specific surface area S_p and pore volume V_p are cited in Table 1.

Results

In Table 1, the specific surface areas S_p ($m^2\ g^{-1}$) calculated according to the BET method and the specific pore volume V_p ($cm^3\ g^{-1}$) calculated from the total nitrogen volume adsorbed are tabulated. In the same table, the maximum D_{max} of the pore size distribution and the variance (2σ) of the distribution is shown. We mention that 2σ corresponds roughly to the full width at half-maximum (fwhm) of the PSD, expressing its narrowness. Finally, the ratio ($D_{max}/2\sigma$) is also cited, which expresses the maximum of the PSD, reduced over the value of 2σ, or otherwise measured with a "stick" equal to 2σ. The surface acidity of the parent SiO_2 was estimated from the TPD/NH_3 experiments to be equal to 12.81×10^{20} sites/g or 4.58×10^{18} sites/m^2. The last value corresponds to an average distance between two acid sites equal to ~5.2 Å (see Figure 1). This is a typical value for acidic silicas. Using the above acid density as the basis of calculation, the proper amount of functionalizing agent(s) was used so as to achieve the various degrees (n) of functionalization (see above, Preparation of Samples). The estimated values of S_p, V_p, D_{max}, 2σ, and $(D_{max}/2\sigma)_{BJH}$ are shown in Figure 6 as a function of the extent of functionalization.

The Calculation of Connectivities *c*. The procedure for the calculation of connectivities c, closely following Seaton,[8] can be summarized as follows: The bond occupation probability f was obtained as a function of the

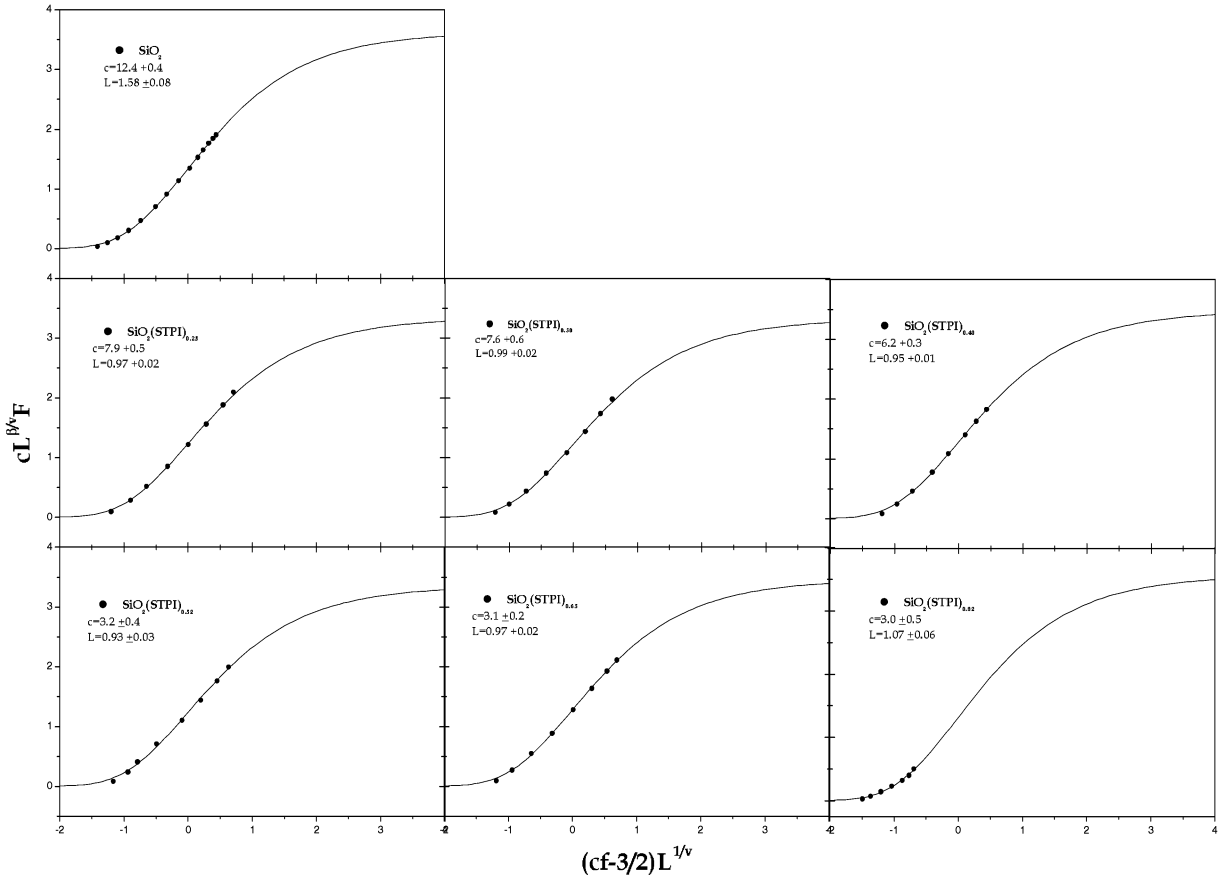

Figure 3. Typical fitting results of eq 7 for the indicated solids and the corresponding *c* and *L* values.

Table 2. Values of Connectivity (*c*), the Characteristic Size of Particles Expressed in Pore Length (*L*), the Dimensionality of Surface Adsorption (D_{sa}), and the Dimensionality of Capillary Condensation D_{cc}

sample	connectivity *c*	characteristic size of particles in porous *L*	dimensionality of surface adsorption D_{sa}	dimensionality of capillary condensation D_{cc}
SiO_2	12.4 ± 0.4	1.58 ± 0.08	2.19	10.43
$SiO_2(STPI)_{0.25}$	7.9 ± 0.5	0.97 ± 0.02	2.21	9.88
$SiO_2(STPI)_{0.30}$	7.6 ± 0.6	0.99 ± 0.02	2.23	8.23
$SiO_2(STPI)_{0.40}$	6.2 ± 0.3	0.95 ± 0.01	2.24	8.17
$SiO_2(STPI)_{0.52}$	3.2 ± 0.4	0.93 ± 0.03	2.26	8.01
$SiO_2(STPI)_{0.60}$	3.1 ± 0.2	0.97 ± 0.02	2.26	7.55
$SiO_2(STPI)_{0.85}$	3.0 ± 0.5	1.07 ± 0.06	2.27	7.51

percolation probability *F* from the adsorption isotherms (Figure 1) using the pore size distribution as follows:

$$f = \frac{\int_{r^*}^{r=\infty} n_r \, dr}{\int_0^{r=\infty} n_r \, dr} \tag{4}$$

$$\frac{F}{f} = \frac{V_{\text{flat max}} - V_{\text{des}}}{V_{\text{flat max}} - V_{\text{ads}}} \tag{5}$$

where n_r is the corresponding PSD using the BJH method for cylindrical pores, $V_{\text{flat max}}$ is the part of desorption curve before the start of desorption, and V_{des} and V_{ads} are the corresponding volumes in the desorption and adsorption curves. Then the best *c* and *L* values are obtained by fitting the experimental scaling data (*F*, *f*) obtained above to generalized scaling relation (6) between *F* and *f*:[22]

$$L^{\beta/\nu} cF = G[(cf - 3/2)L^{1/\nu}] \tag{6}$$

where *c* is connectivity and *L* is the so-called characteristic size of particles that expresses the number of pore lengths.

In our analysis, the generalized scaling relation (6) was constructed using the critical exponents $\beta = 0.41$ and $\nu = 0.88$ given by Kirkpatrick.[22] Typical fitting results are shown in Figure 3. The calculated *c* and *L* values are in Table 2. The *c* values as a function of degree *n* of functionalization are shown in Figure 6.

The Estimation of Dimensionality of Surface Adsorption D_{sa} and of Capillary Condensation D_{cc}. The calculation of the dimensionality of surface adsorption D_{sa} and the dimensionality of the capillary condensation D_{cc} took place using the thermodynamic approach (eq 3). For the calculation of D_{sa} and D_{cc} values according to eq 3, the drawn lines are in Figure 4. Those lines show at least two distinct slopes, one at low P/P_0, and another at higher P/P_0. From these slopes, two *D* values were calculated and designated as D_{sa} (meaning dimensionality of surface adsorption) and D_{cc} (meaning dimensionality of capillary condensation). Those values, D_{sa} and D_{cc}, are included in Table 2 and are shown as a degree of

(22) Kirkpatrick, S. *III−Condensed Matter*; Ballian, R., Mayward, R., Toulouse, G., Eds.; North-Holland: Amsterdam, 1979.
(23) Brunauer, S.; Emmett, P. H.; Teller, E. *J. Am. Chem. Soc.* **1938**, *60*, 309.

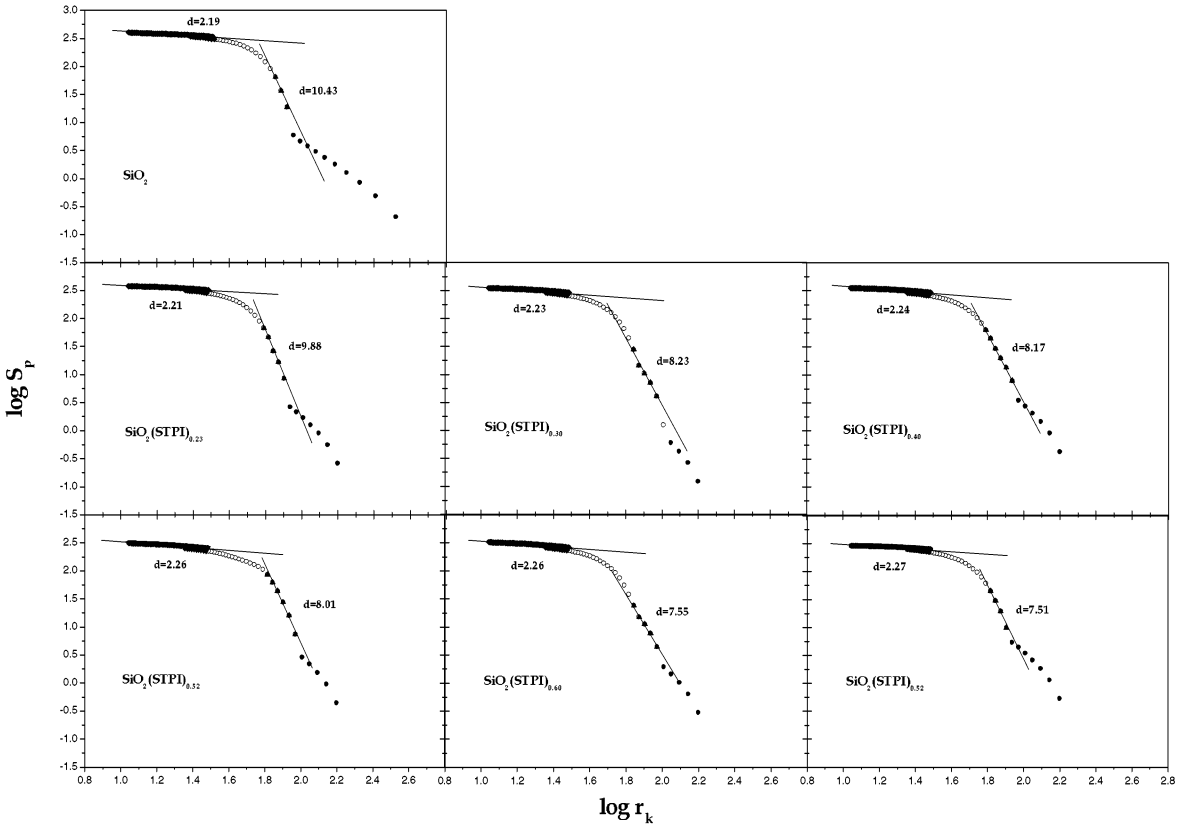

Figure 4. Estimation of D_{as} and D_{cc} parameters using eq 3.

functionalization n in Figure 6. We draw attention to the fact that D_{cc} values reflect only the dimensionality of condensation in the capillary and have nothing to do with the dimensionality of the surface adsorption process.[10]

Simulation of Nitrogen Sorption Data Using the CPSM. Additionally to the above, the CPSM[13,15,16] was employed to simulate the N_2 adsorption−desorption experimental data. The intention is to work out true PSD curves based on a simulation of the *entire hysteresis loop* and to use a single PSD prediction and thus to *overcome the difficulty of choosing either one or the other branch of hysteresis loops*, which result in dissimilar predictions.

The PSD predicted by the CPSM model (i.e., solid line PSDs in Figure 5) indicates D_{max} values that approach those deduced by the BJH method. Cumulative pore volumes calculated by the CPSM predicted PSDs which are in satisfactory agreement with those evaluated directly from the adsorption isotherm data.

The CPSM simulation also helps in extracting additional pore structure information, for example, the nominal pore length N_s that enables the estimation of the pore structure tortuosity factors.[15]

A detailed description of the CPSM model and how it is applied for the simulation of the N_2 adsorption−desorption loop, the estimation of the PSD, and the calculation of empirical tortuosity factors τ can be found in the original papers.[13,15,16] The CPSM simulation results for all materials dealt with in this work are depicted in Figure 5. Values of the CPSM fitting parameters for each particular material studied are tabulated in Table 3.

The PSD_{CPSM} data were then used to evaluate the mean pore size D_{mean}, the effective minimum and maximum of the pore sizes, that is, $D_{min,eff}$ and $D_{max,eff}$, which were then utilized to calculate tortuosity factors τ via the empirical correlation

$$\tau_{CPSM} = 1 + 0.69\left(\frac{D_{max,eff} - D_{min,eff}}{D_{mean}}\right)(N_s - 2)^{0.58} \quad (7)$$

The corresponding D_{mean}, $D_{max,eff}$, and $D_{min,eff}$ and the τ values are collected in Table 4.

The various parameters calculated via classical/standard methods and those found via the CPSM methodology are depicted in Figure 6 as a function of degree of functionalization n for comparison. This figure includes the calculated surface areas S_p and S_{CPSM}, the pore volumes V_p and V_{CPSM}, the mean pore connectivity c, the dimensionality of capillary condensation D_{cc}, the tortuosity factor τ, the D_{max} of the PSD, the variance 2σ of the PSD, and finally the corresponding ratio ($D_{max}/2\sigma$). In the following discussion, we shall discuss first how those parameters are affected by the degree n of functionalization, next how they are interrelated, and finally some discrepancies observed between values calculated via the classical and the CPSM methods.

Discussion

The gradual functionalization of the surface of SiO_2 with the STPI groups results in a gradual decrease of surface areas S_p and the pore volume V_p of the solids as shown graphically in Figure 6. In the same figure, the variation of other parameters such as connectivity c, dimensionality of capillary condensation D_{cc}, the D_{max} and the variance 2σ of the PSD, the ratio ($D_{max}/2\sigma$), and the tortuosity τ are shown as a function of degree of functionalization n.

Various interesting observations can be made from this figure. Perhaps the most trivial and predictable is the almost linear decrease of surface area S_p and pore volume V_p with the degree of functionalization (see Figure 6a,b).

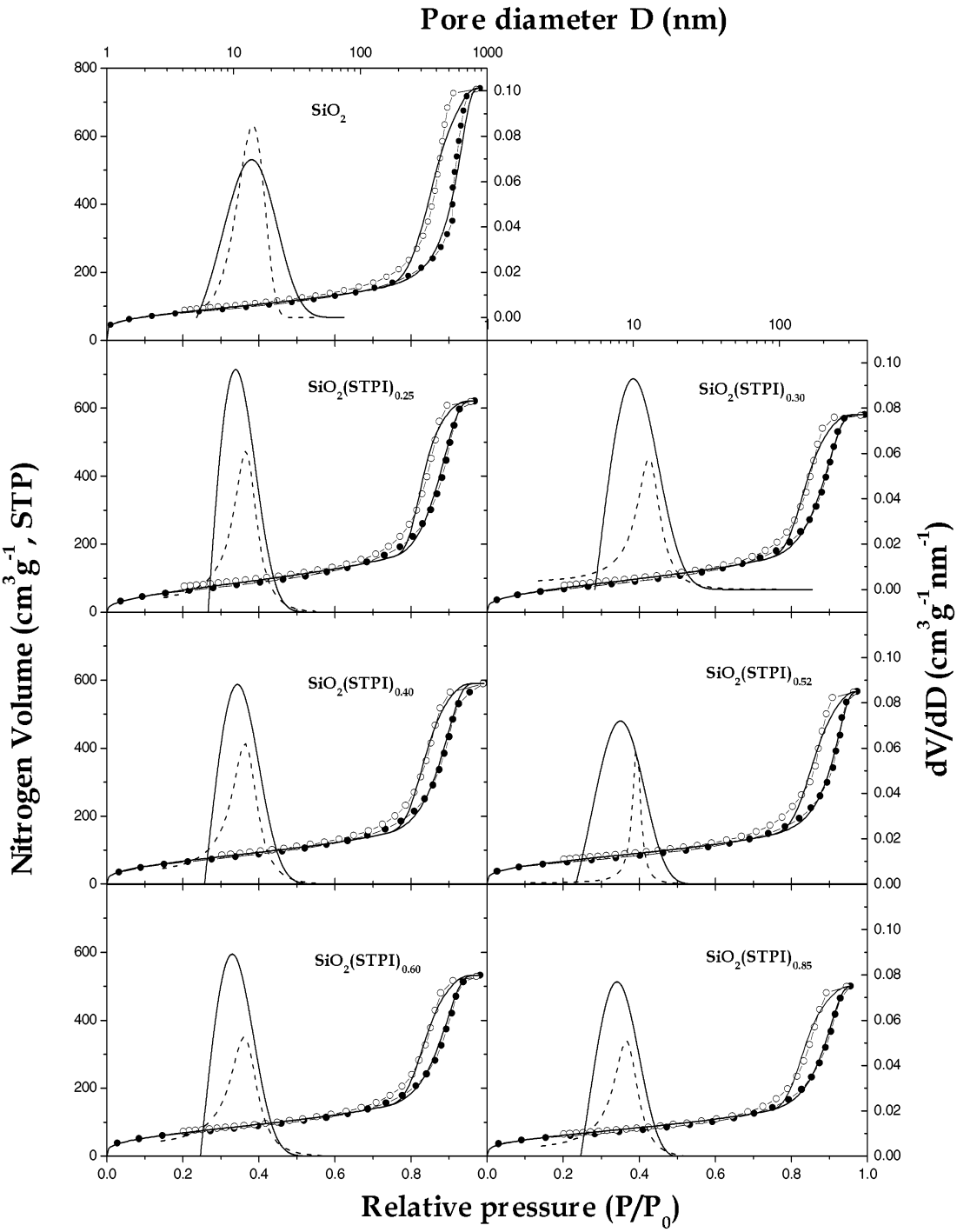

Figure 5. CPSM simulation of N_2 adsorption/desorption hysteresis data. The points (○ and ●) are experimental, and the bold line is fitting by the CPSM. The intrinsic pore volume distributions generated from the CPSM analysis of the N_2 sorption data are shown by the continuous line. With the dashed line, the distribution obtained using the desorption loop as in Figure 2 is also shown.

Clearly the STPI groups having a length of around ~8 Å (see Figure 1) block various micropores, to a total or partial extent, so the remaining area and the volume available for N_2 adsorption are substantially lower. Since $n = 1$ actually corresponds to the introduction of STPI groups to the total number of acid sites $N = 12.8 \times 10^{20}$/g, it can be easily estimated for the results in Figure 6a,b that there is a loss of 7.0 Å^2 of surface area per STPI group, which is a very reasonable result. On the other hand, there is a loss of 350 Å^3 pore volume per STPI group. This last value indicates the more dramatic effect of functionalization in blocking the previously accessible pore volume compared to the effect on the surface area. Clearly the STPI groups block the mouths of pores and this also affects the connectivity of the system.

The effect of functionalization on the D_{max} of the PSD is as expected, in the sense that D_{max} tends to lower values (see Figure 6g). There is an exception with the point at $n = 0.52$ which shows abnormally high D_{max} values. This point appears also out of trend in other cases (see Figure 6e,f) for reasons which are not clear. The decrease of D_{max} reflects the overall narrowing of pores.

But at the same time, the effect of functionalization on the variance (2σ) of the PSD is rather peculiar. In other words, 2σ *initially decreases* with n and *subsequently increases* (see Figure 6h). At first glance, this means that

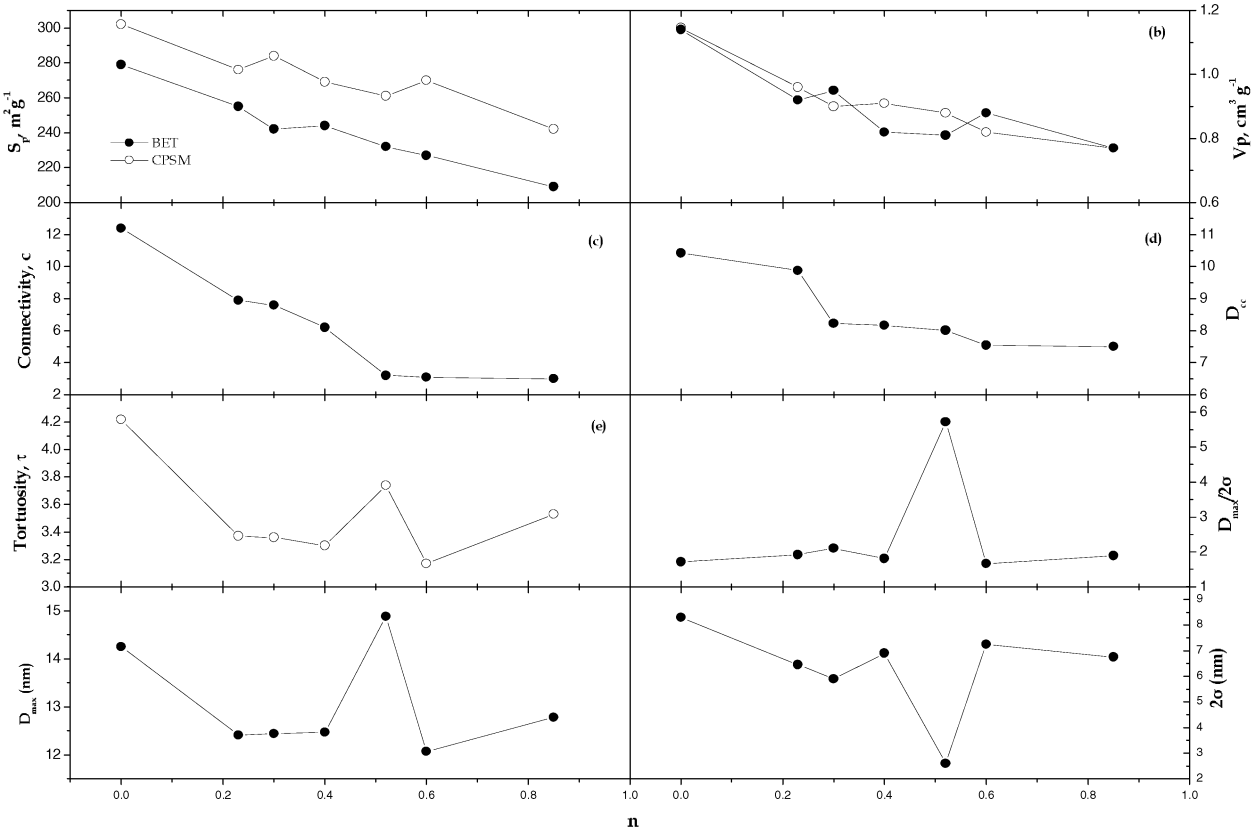

Figure 6. Variation of parameters S_p, V_p, V_{CPSM}, c, D_{cc}, τ, D_{max}, 2σ, and $D_{max}/2\sigma$ with the degree n of surface functionalization. Open symbols were deduced from CPSM analysis.

Table 3. CPSM Fitting Parameters Corresponding to the Simulations Shown in Figure 5

		pore number distribution $F(D)$ characterization parameters			Kelvin[b] parameters		parameters of t (nm), eq I-1	
specimen	N_s[a]	b_1	P_{ce}/P_0	$(P/P_0)_{max}$	cos θ_c	cos θ_h	m	n
SiO_2	8.5	−18	0.70	0.9824	0.65	0.65	0.10	0.35
$SiO_2(STPI)_{0.23}$	8.0	−18	0.75	0.9675	0.70	0.70	0.30	0.35
$SiO_2(STPI)_{0.30}$	7.0	−70	0.73	0.9926	0.63	0.63	0.22	0.35
$SiO_2(STPI)_{0.40}$	6.8	−68	0.73	0.9921	0.70	0.70	0.22	0.35
$SiO_2(STPI)_{0.52}$	7.8	−13	0.73	0.9732	0.55	0.55	0.18	0.35
$SiO_2(STPI)_{0.60}$	6.5	−30	0.73	0.9821	0.63	0.63	0.20	0.35
$SiO_2(STPI)_{0.85}$	8.5	−10	0.73	0.9559	0.63	0.63	0.20	0.35

[a] CPSM nominal pore length. [b] As defined by eq 11 (ref 17).

Table 4. Tabulation of Tortuosity Factor τ Data for the Functionalized Mesoporous Silicas[a]

specimen	$S_{CPSM,mu}$ $m^2\ g^{-1}$	V_{CPSM} $cm^3\ g^{-1}$	$D_{min,eff}$ nm	$D_{max,eff}$ nm	D_{mean} nm	τ_{CPSM}
SiO_2	305	1.15	7.33	35.39	17.80	4.22
$SiO_2(STPI)_{0.23}$	327	0.96	7.26	22.91	12.89	3.37
$SiO_2(STPI)_{0.30}$	317	0.90	6.53	23.53	12.64	3.36
$SiO_2(STPI)_{0.40}$	301	0.91	7.03	25.27	13.57	3.30
$SiO_2(STPI)_{0.52}$	283	0.88	6.52	26.80	14.16	3.74
$SiO_2(STPI)_{0.60}$	297	0.82	6.49	22.69	12.31	3.17
$SiO_2(STPI)_{0.85}$	267	0.77	6.66	22.61	12.86	3.53

[a] Predictions made by the CPSM-tortuosity model.

the PSD is initially getting narrower with the progress of functionalization and then tends to widen again. Actually this phenomenon is more complex and is due to the initial lowering of the height of the PSD with the increase of functionalization. This lowering of the whole PSD results also in lowering its full width at half-maximum, fwhm $\sim 2\sigma$. As a result of the simultaneous decrease of D_{max} and the initial decrease of 2σ, their ratio $D_{max}/2\sigma$ is approximately constant with the progress of functionalization as seen in Figure 6f.

The gradual functionalization results in lowering the mean connectivity of the porous network. Indeed as shown in Figure 6c, the connectivity c drops almost linearly from $c = 12.4$ to $c = 3.1$ as the STPI addition increases from $n = 0$ to $n = 0.6$. Then further functionalization ($n = 0.8$) does not seem to affect c, which remains steady at $c = 3.0$. Similar results showing a decrease of connectivity from $c \sim 11$ to $c \sim 6$ by the process of functionalization of SiO_2 with *n*-octadecyl-dimethyl-monochlorosilane have been reported by Liapis.[9] We draw attention to the fact that the algorithm used by Liapis for the estimation of c is different to the one proposed by Seaton and employed in the present study, so the results in this paper cannot be quantitatively compared with the ones in ref 9.

The D_{cc} values, corresponding to the dimensionality of capillary condensation, drop from $D_{cc} = 10.43$ at $n = 0$ to $D_{cc} = 8.23$ at $n = 0.30$ and then decrease more slowly as $n \rightarrow 8.5$ (see Figure 6d). The D_{cc} values are usually high when pore size is uniform and the corresponding PSD is narrow, that is, like the MCM solids.[10] Conversely, the D_{cc} values are small when the PSD is more spread and the 2σ values are large.[20] Therefore it is not strange that as

2σ increases (see Figure 6h) and/or the $D_{max}/2\sigma$ drops (see Figure 6f) the D_{cc} value drops (Figure 6d). A numerical correlation between those quantities, D_{cc} and 2σ or D_{cc} and $D_{max}/2\sigma$, is not appropriate in the present case because of the limited number of points, but some remarkable correlation for a large number of mesoporous aluminophosphates is given in refs 10 and 20.

Another interesting point is also the appreciable drop of tortuosity τ occurring at the beginning of surface functionalization ($n = 0.23$) while this decrease becomes almost negligible at higher ($n > 0.23$) values (see Figure 6e). The initial decrease of τ reflects the overall phenomenon of pore structure alteration due to functionalization. Higher τ values are normally associated with wider hysteresis loops provided that there is no substantial interference of capillary condensation metastability effects that can give rise to enhanced hysteresis phenomena and wider hysteresis loops. But clearly this is not the case here; the adsorption/desorption loops are getting rather smaller (see Figure 1), which means that the STPI functionalization does not result in the development of additional hysteresis.

The Correlation between D_{cc} and c. As seen by comparing parts c and d of Figure 6, the connectivity, c, and dimensionality of capillary condensation, D_{cc}, both decrease with n. A first-order correlation between them is $D_{cc} = 6.69 + 0.3c$ with a correlation factor $R = 0.90$ which is better than a 95% confidence limit. This relation conveys the fact that the process of gradual and controlled narrowing of pores by the addition of STPI groups affects both D_{cc} and c in the same direction. But this is not actually the case for random porous networks in solids left to developed "freely" from the thermodynamic point view without imposing on them any post priori "functionalization". Thus in ref 10, which referred to 16 mesoporous vanado-phosphoro-aluminates, it was shown that high D_{cc} values correspond to low connectivity and vice versa. But those solids[10] possess random porous networks developed freely under normal drying conditions, which allow the structure to develop in a relaxed way. If in such a random porous material, like the original SiO_2 employed in this work, we start imposing post priori functionalization, then this has the effect shown by eq 11.

Finally, we should add a comment about the difference observed between the specific surface areas S_p and S_{CPSM} as shown in Table 4 and depicted in Figure 6a. Evidently, a clear drop of S_{CPSM} with respect to the degree of functionalization (n) was observed and this drop moves parallel to the drop of S_p. The S_{CPSM} values are higher by 26−75 $m^2\ g^{-1}$, which is 8−23% higher than the corresponding S_p ones. We attribute this misfitting to some kind of overestimation of monolayer volume V_m by the CPSM. Namely, since ssa $= 4.536V_m$ it follows that an overestimation of V_m by 5−17 cm^3 N_2/g results in the mentioned discrepancy. Probably the CPSM algorithm results in some kind of mismatching with the experimental results, resulting in higher values of adsorbed nitrogen. Such discrepancies do not appear between V_p and V_{CPSM}, since the essence of the fitting is exactly the matching of the whole experimental results with the CPSM-calculated adsorption−desorption volumes of nitrogen.

Conclusions

The gradual functionalization of a commercial SiO_2 with silano-(trimethoxy)-propyl-imidazole groups to an extent equal to $n = 0.00$, 0.23, 0.30, 0.40, 0.52, 0.60, and 0.85 of its surface acid sites results in a gradual drop of the specific surface area S_p ($m^2\ g^{-1}$) from ∼280 to 210 $m^2\ g^{-1}$ and of the specific pore volume V_p ($cm^3\ g^{-1}$) of the original material from 1.14 to 0.77 $cm^3\ g^{-1}$. The D_{max} of the PSD moves to lower values while the variance 2σ of the distribution remains almost constant. The mean connectivity c of the porous network, calculated according to the method of Seaton, drops from $c \sim 12.4$ at $n = 0$ to $c \sim 3.0$ at $n = 0.85$. A similar decreasing path is followed also by the dimensionality of capillary condensation, D_{cc}, from $D_{cc} = 10.4$ at $n = 0$ to $D_{cc} = 7.5$ at $n = 0.85$. The tortuosity τ of the seven samples, calculated according to the CPSM, also appears to drop, presumably because of blocking of various pore channels. The same CPSM model provides pore volume values V_{CPSM} which are practically identical to the ones calculated using the classical method (V_p). The specific surface area S_{SPCM} found via the CPSM simulation is 8−23% higher than the S_p values found using the BET method applied to the experimental data. This is due to some overestimation of N_2 adsorption volume in the range $P/P_0 = 0.05-0.25$ by the CPSM algorithm. It seems that the CPSM model can be used as an additional method for enriching the data we can extract from N_2 adsorption/desorption measurements with the values of the mean tortuosity (τ) of solids with random porous networks. The interrelationship between connectivity c and tortuosity τ is not clear for the moment, but there are indications that they move in the same direction, at least in the ranges examined in this work. Finally, we should draw attention to the fact that the post priori functionalization of a random porous network affects the interrelation between parameters such as connectivity c and the D_{cc} in a different way than the one found in a porous system possessing a random porous network and developed freely under conditions of thermodynamic equilibrium.

LA020261H